ChemComm

Accepted Manuscript

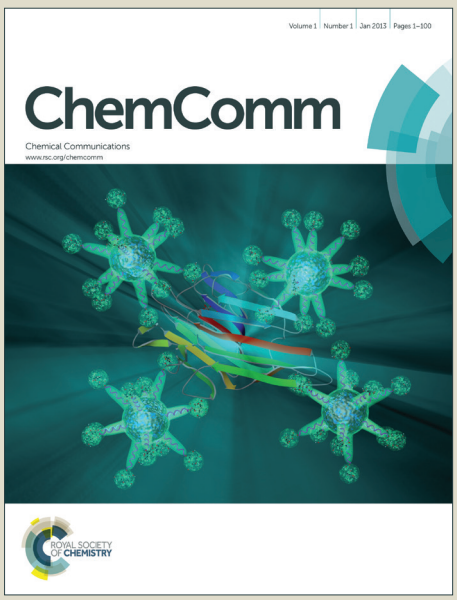

ROYAL SOCIETY OF CHEMISTRY

www.rsc.org/chemcomm

Journal Name

RSCPublishing

COMMUNICATION

SnSe alloy as a promising anode material for Na-ion batteries

Cite this: DOI: 10.1039/x0xx00000x

Youngjin Kim,[a] Yongil Kim,[a] Yuwon Park,[a] Yong Nam Jo,[b] Young-Jun Kim,[b] Nam-Soon Choi,[a] and Kyu Tae Lee*[a]

Received 00th January 2012,
Accepted 00th January 2012

DOI: 10.1039/x0xx00000x

www.rsc.org/

SnSe alloy is first examined as an anode for Na-ion batteries, and shows excellent electrochemical performance including a high reversible capacity of 707 mA h g^{-1} and stable cycle performance over 50 cycles. On sodiation, SnSe is changed into amorphous Na_xSn nanodomains dispersed in crystalline Na_2Se, and SnSe is reversibly restored after desodiation.

In recent years, the demand for large scale energy storage devices has increased with the development of electric vehicles (EVs) and the smart grid, and Li-ion batteries are considered promising candidates because of their high energy density.[1] However, there is growing concern that lithium resources are insufficient to meet the demands of large scale applications. Moreover, the recent price of lithium raw materials has shown sharp increases. Cosquently, Na-ion batteries are an alternative to Li-ion batteries because sodium resources are much more abundant and inexpensive than lithium.[2] However, there is a critical obstacle to their development. The energy density of Na-ion batteries is slightly lower than that of Li-ion batteries because the reversible capacity and operating voltage of currently reported electrode materials in Na-ion batteries are lower in comparison. This implies that it is not easy to replace Li-ion batteries with Na-ion batteries because the cost per energy stored ($/Wh) of Na-ion batteries does not provide much advantage.[3] Therefore, new electrode materials having higher reversible capacities are necessary if one is to increase the energy density of Na-ion batteries.

Recently, there have been notable achievements in developing high-capacity anode materials such as phosphorus,[4] phosphides,[5] oxides,[6] sulfides,[7] selenides[8] and alloy-based materials such as Sn[9] and Sb[10]. In particular, Sn-based materials have been a focus as promising anode materials. Sn is easily reacted with group VA elements (pnictogens including N, P, and Sb) and group VIA elements (chalcogens including O, S, and Se) to form binary compounds such as pnictogenides and chalcogenides. Among these binary compounds, SnSb,[11] SnO_2,[12] SnS_2,[13] and Sn_4P_3[5a, 5b] have been examined, and show promising electrochemical performance via conversion reactions forming $Na_\alpha Sn$ and $Na_\beta X$ (X = pnictogens or chalcogens) during sodiation. In the case of tin nitride, it was calculated that the conversion reaction with Na is not thermodynamically allowed.[14] Tin selenide, however, has not been examined as an anode for Na-ion batteries. SnSe is a p-type semiconductor (band gap of 0.9-1.3 eV) with an orthorhombic crystal structure. In SnSe, Se is more electronegative than Sn whose oxidation state is +2.[15]

In this study, SnSe was for the first time examined as an anode material for Na-ion batteries, although a few studies have reported the electrochemical reaction mechanism of SnSe for Li-ion batteries.[16] SnSe showed excellent electrochemical performance for Na-ion batteries, including a high reversible capacity of 707 mA h g^{-1} and very stable cycle performance with negligible capacity fading over 50 cycles.

SnSe/C composite powders were obtained via facile ball milling in an Ar atmosphere using tin selenide and Super P carbon with a weight ratio of 7:3. **Figure 1a** shows the X-ray diffraction (XRD) pattern of as-prepared SeSe/C powders; no impurities were observed. The space group of the SnSe crystal structure is *Pnma*, and SnSe crystallizes in a orthorhombic lattice. A Raman spectrum of the SnSe/C composite shows that Super P carbon in the composite is a disordered carbon (**Fig. 1b**), where the two peaks around1350 and 1580 cm^{-1} are designated as D and G bands, respectively. **Figure 1c** shows a field emission scanning electron microscopy (FE-SEM) image of the SnSe/C composite powders. Primary particles with sizes tens of nm were aggregated to form secondary particles with sizes hundreds of nm. Scanning transmission electron microscopy (STEM) and energy dispersive X-ray spectroscopy (EDS) mapping images of the SnSe/C composite indicate that SnSe and carbon are homogeneously mixed at the nanoscale level (**Fig. 1d**).

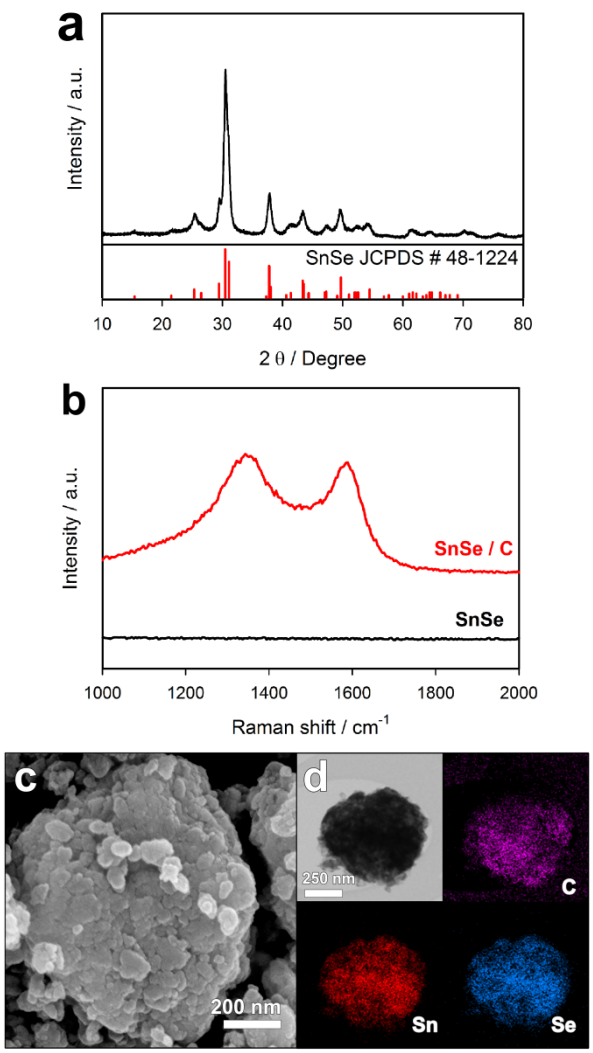

Fig. 1 (a) X-ray diffraction pattern of SnSe/C (b) Raman spectra of SnSe/C (red line) and bare SnSe (black line) (c) FE-SEM image and (d) STEM image and EDS mapping images of carbon, tin, and selenium.

Electrochemical performance of the SnSe/C composite was evaluated using a half cell with a sodium metal electrode at a current density of 143 mA g^{-1} (~0.2C). **Figure 2a** shows the cycle performance of the SnSe/C composite, exhibiting negligible capacity fading over 50 cycles. Its reversible capacity is 707 mA h g^{-1}, delivering 91% of the theoretical capacity of SnSe (780 mA h g^{-1}). This calculation assumes that SnSe is changed into Na_2Se and $Na_{15}Sn_4$ during sodiation. The coulombic efficiency at the first cycle was 75.3 %. **Figure 2b** shows galvanostatic voltage profiles of the SnSe/C electrode. The sodiation profile is characterized by two regions including a plateau located at about 0.9 V and a sloping profile between 0.6 and 0 V, which is clearly shown in the differential capacity (dQ/dV) plots (**Fig. 2c**). The peak area (corresponding to capacity) around 0.9 V for the first cycle decreased after subsequent cycling. This indicates that the plateau at 0.9 V for the first cycle is attributable to irreversible electrolyte decomposition such as occurs through the formation of a solid electrolyte interphase (SEI). However, the small hump around 1 V was still observed at the 10th cycle, suggesting that the plateau at 0.9

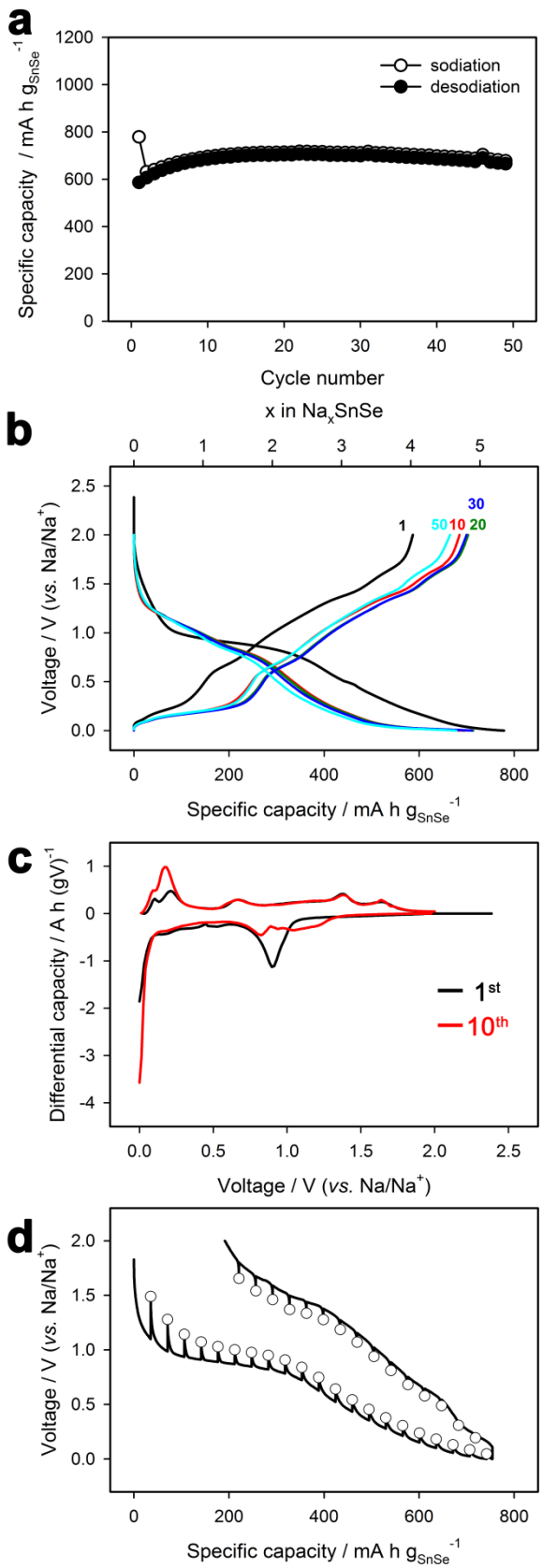

Fig. 2 (a) Cycle performance, (b) Voltage profiles, (c) Differential capacity (dQ/dV) plots, and (d) GITT profiles of SnSe/C

V for the first cycle includes not only irreversible electrolyte decomposition but also reversible (de)sodiation. Furthermore, the rate performance of the composite was examined, and it delivered about 350 mA h g^{-1} at 1C rate (**Fig. S1**).

In order to elucidate the (de)sodiation mechanism of SnSe/C during charge/discharge, *ex situ* XRD analysis of the SnSe/C was performed at various degrees of state of charge (SOC) in the first cycle (**Fig. 3**). It revealed that sodiation of the SnSe/C proceeds in two consecutive reactions. As approaching the redox potential of 0.6 V vs. Na/Na^+, the formation of crystalline Na_2Se and Sn were observed with the disappearance of SnSe, as shown in **Fig. 3 (ii)**. This indicates that the plateau at 0.9 V is attributed to the two-phase reaction for conversion of SnSe into Na_2Se and Sn. After full sodiation (at 0 V), the XRD peaks of Sn disappeared, and only those of Na_2Se were observed (**Fig. 3 (iii)**). This indicates that the amorphous Na_xSn phase was formed via the sodiation between 0.6 and 0 V. This is the one-phase reaction, because a sloping voltage profile was observed in this region, as shown in the quasi-open-circuit voltage (QOCV) profile obtained via a galvanostatic intermittent titration technique (GITT) (**Fig. 2d**). After full desodiation (at 2 V), a small broad XRD peak near 31° corresponding to SnSe was observed, indicating that SnSe was reversibly restored from Na_xSn and Na_2Se (**Fig. 3 (v)**). The (de)sodiation mechanism of SnSe is summarized, as follows:

Sodiation:

Step 1: $SnSe + 2Na^+ + 2e^- \rightarrow$ *c*-Sn + *c*-Na_2Se (1)

Step 2: *c*-Sn + $xNa^+ + xe^-$ + *c*-$Na_2Se \rightarrow$ *a*-Na_xSn + *c*-Na_2Se (2)

Desodiation:

a-Na_xSn + *c*-$Na_2Se \rightarrow SnSe + (2+x)Na^+ + (2+x)e^-$ (3)

(*a*: amorphous, *c*: crystalline)

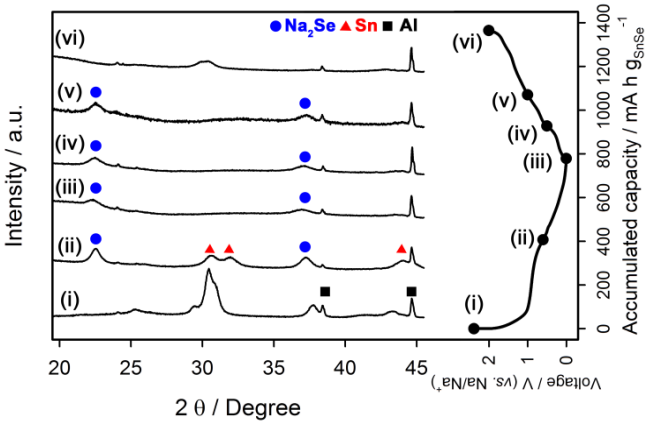

Fig. 3 *Ex situ* XRD patterns of the SnSe/C composite electrode collected at various points as indicated in the corresponding voltage profile: (i) pristine, (ii) 0.6 V, (iii) 0 V, (iv) 0.5 V, (v) 1 V, and (vi) 2 V.

Further support for the (de)sodiation mechanism of the SnSe/C was given by the *ex situ* TEM analysis combined with EDS mapping images. **Figure 4a** shows the bright-field TEM and EDS mapping images of the fully sodiated SnSe/C electrode. After full sodiation (at 0 V), Na_xSn domains (dark region) with sizes between tens of and a few hundred nm dispersed in the Na_2Se matrix (bright region) were observed, which is clearly supported by the EDS mapping images for the elements of Sn, Se, and Na. After full desodiation, the segregated Sn domains disappeared, and homogenously-overlapped EDS maps for Sn and Se were observed (**Fig. 4b**). This indicates

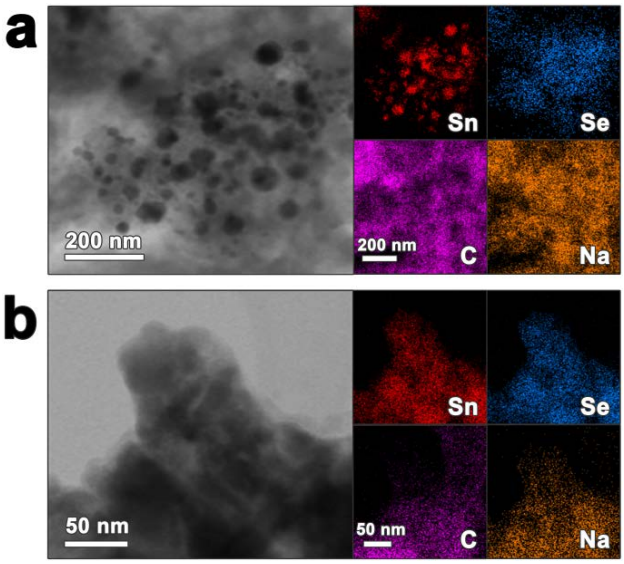

Fig. 4 The STEM images and EDS elemental mapping of tin, selenium, carbon, and sodium of fully (a) sodiated and (b) desodiated SnSe/C.

that SnSe was reversibly formed after full desodiation. Relatively weak EDS intensity from Na was also observed even after desodiation; this is attributed to SEI layers containing Na. In addition, it is considered that the morphology change showing the confinement of Na_xSn domains in the Na_2Se matrix was critical in the better cycle performance of SnSe compared to previous reports for Sn.[9] It is well-known that the pulverization or cracking of Sn is caused by the agglomeration of Sn particles during cycling, resulting in capacity fading of Sn electrodes. However, in the case of SnSe, Sn or NaxSn domains were embedded in the Na_2Se matrix during cycling, and thus agglomeration of Sn is inhibited, leading to enhanced cycle performance. Moreover, the cycle performance of pure Sn is dependent on its operating voltage range because the electrolyte decomposition is accelerated at > 0.8 V vs. Na/Na^+.[9a] Therefore, pure Sn showed poor cycle performance in the voltage range of 0-1.5 V vs. Na/Na^+. However, pure Se exhibited excellent cycle performance better than pure Sn, indicating the electrolyte decomposition on the surface of Se is not as severe as that of Sn.[17] In the case of SnSe, the surface of Sn is not exposed to electrolytes because of Sn or Na_xSn domains embedded in the Na_2Se matrix, and this results in the alleviated electrolyte decomposition of SnSe. Therefore, the better cycle performance of SnSe than pure Sn is partially attributed to that the surface of Se is exposed to electrolytes.

In summary, a SnSe/C composite was obtained through facile ball milling, and we demonstrated, for the first time, its electrochemical performance as an anode material for Na-ion batteries. SnSe/C is remarkable as a promising anode candidate for Na-ion batteries because of its reversible specific capacity. In this study, SnSe/C showed excellent electrochemical performance including a high reversible capacity of 707 mA h g^{-1} and excellent cycle performance with negligible capacity fading over 50 cycles. The improved cycle performance of SnSe/C was attributed to the confinement effect of Na_xSn domains in the Na_2Se matrix during cycling. In addition, the reversible (de)sodiation mechanism of SnSe was established through *ex situ* XRD and TEM with EDS analyses. It is believed that understanding this reaction mechanism of SnSe will contribute to developing alloy-based materials for Na-ion batteries.

Acknowledgement

This research was supported by the National Research Foundation of Korea (NRF) grant funded by the Korea Government (MSIP and MOE) (No. 2010-0019408 and No. NRF-2013R1A1A2013446), and by Korea Electrotechnology Research Institute (KERI) Primary research program through the National Research Council of Science & Technology funded by the Ministry of Science, ICT and Future Planning (MSIP) (No. 14-12-N0101-69).

Notes and references

[a] School of Energy and Chemical Engineering, Ulsan National Institute of Science and Technology (UNIST), 100 Banyeon-ri, Eonyang-eup, Ulju-gun, Ulsan, 689-798 (South Korea) E-mail: ktlee@unist.ac.kr, Fax: +82-52-217-3009, Tel: +82-52-217-2930.

[b]Advanced Batteries Research Center, Korea Electronics Technology Institute (KETI), 68 Yatap-dong, Bundang-gu, Seongnam-si, Gyeonggi-do, 463-816 (South Korea)

† Electronic Supplementary Information (ESI) available: Experimental section. See DOI: 10.1039/c000000x/

1 (a) M. Armand and J. M. Tarascon, *Nature*, 2008, **451**, 652; (b) N.-S. Choi, Z. Chen, S. A. Freunberger, X. Ji, Y.-K. Sun, K. Amine, G. Yushin, L. F. Nazar, J. Cho and P. G. Bruce, *Angew. Chem. Int. Ed.*, 2012, **51**, 9994; (c) B. L. Ellis, K. T. Lee and L. F. Nazar, *Chem. Mater.*, 2010, **22**, 691.

2 (a) B. L. Ellis and L. F. Nazar, *Curr. Opin. Solid State Mater. Sci.*, 2012, **16**, 168; (b) S.-W. Kim, D.-H. Seo, X. Ma, G. Ceder and K. Kang, *Adv. Energy Mater.*, 2012, **2**, 710; (c) S. Y. Hong, Y. Kim, Y. Park, A. Choi, N.-S. Choi and K. T. Lee, *Energy Environ. Sci.*, 2013, **6**, 2067; (d) V. Palomares, P. Serras, I. Villaluenga, K. B. Hueso, J. Carretero-Gonzalez and T. Rojo, *Energy Environ. Sci.*, 2012, **5**, 5884; (e) M. D. Slater, D. Kim, E. Lee and C. S. Johnson, *Adv. Funct. Mater.*, 2013, **23**, 947; (f) H. Pan, Y.-S. Hu and L. Chen, *Energy Environ. Sci.*, 2013, **6**, 2338.

3 Y. Kim, K.-H. Ha, S. M. Oh and K. T. Lee, *Chem. Eur. J.*, 2014, **20**, 11980.

4 (a) Y. Kim, Y. Park, A. Choi, N.-S. Choi, J. Kim, J. Lee, J. H. Ryu, S. M. Oh and K. T. Lee, *Adv. Mater.*, 2013, **25**, 3045; (b) J. Qian, X. Wu, Y. Cao, X. Ai and H. Yang, *Angew. Chem. Int. Ed.*, 2013, **52**, 4633; (c) N. Yabuuchi, Y. Matsuura, T. Ishikawa, S. Kuze, J.-Y. Son, Y.-T. Cui, H. Oji and S. Komaba, *ChemElectroChem*, 2014, **1**, 580; (d) W.-J. Li, S.-L. Chou, J.-Z. Wang, H.-K. Liu and S.-X. Dou, *Nano Lett.*, 2013, **13**, 5480.

5 (a) Y. Kim, Y. Kim, A. Choi, S. Woo, D. Mok, N. S. Choi, Y. S. Jung, J. H. Ryu, S. M. Oh and K. T. Lee, *Adv Mater*, 2014, **26**, 4139; (b) J. Qian, Y. Xiong, Y. Cao, X. Ai and H. Yang, *Nano Lett.*, 2014, **14**, 1865; (c) W. Li, S.-L. Chou, J.-Z. Wang, J. H. Kim, H.-K. Liu and S.-X. Dou, *Adv. Mater.*, 2014, **26**, 4037; (d) J. Fullenwarth, A. Darwiche, A. Soares, B. Donnadieu and L. Monconduit, *J. Mater. Chem. A*, 2014, **2**, 2050.

6 (a) S. Yuan, X.-l. Huang, D.-l. Ma, H.-g. Wang, F.-z. Meng and X.-b. Zhang, *Adv. Mater.*, 2014, **26**, 2273; (b) S. Hariharan, K. Saravanan, V. Ramar and P. Balaya, *Phys. Chem. Chem. Phys.*, 2013, **15**, 2945; (c) B. Koo, S. Chattopadhyay, T. Shibata, V. B. Prakapenka, C. S. Johnson, T. Rajh and E. V. Shevchenko, *Chem. Mater.*, 2012, **25**, 245; (d) M. C. Lopez, P. Lavela, G. F. Ortiz and J. L. Tirado, *Electrochem. Commun.*, 2013, **27**, 152; (e) M. M. Rahman, A. M. Glushenkov, T. Ramireddy and Y. Chen, *Chem. Commun.*, 2014, **50**, 5057; (f) M. Valvo, F. Lindgren, U. Lafont, F. Björefors and K. Edström, *J. Power Sources*, 2014, **245**, 967.

7 (a) G. S. Bang, K. W. Nam, J. Y. Kim, J. Shin, J. W. Choi and S.-Y. Choi, *ACS Appl. Mater. Interfaces*, 2014, **6**, 7084; (b) L. David, R. Bhandavat and G. Singh, *ACS Nano*, 2014, **8**, 1759; (c) D. Y. Yu, P. V. Prikhodchenko, C. W. Mason, S. K. Batabyal, J. Gun, S. Sladkevich, A. G. Medvedev and O. Lev, *Nat. Commun.*, 2013, **4**, 2922; (d) C. Zhu, X. Mu, P. A. van Aken, Y. Yu and J. Maier, *Angew. Chem. Int. Ed.*, 2014, **53**, 2152; (e) Y.-X. Wang, K. H. Seng, S.-L. Chou, J.-Z. Wang, Z. Guo, D. Wexler, H.-K. Liu and S.-X. Dou, *Chem. Commun.*, 2014, **50**, 10730.

8 Y. N. Ko, S. H. Choi, S. B. Park and Y. C. Kang, *Nanoscale*, 2014, **6**, 10511.

9 (a) S. Komaba, Y. Matsuura, T. Ishikawa, N. Yabuuchi, W. Murata and S. Kuze, *Electrochem. Commun.*, 2012, **21**, 65; (b) Y. Xu, Y. Zhu, Y. Liu and C. Wang, *Adv. Energy Mater.*, 2013, **3**, 128; (c) L. D. Ellis, T. D. Hatchard and M. N. Obrovac, *J. Electrochem. Soc.*, 2012, **159**, A1801; (d) J. W. Wang, X. H. Liu, S. X. Mao and J. Y. Huang, *Nano Lett.*, 2012, **12**, 5897; (e) Y. Liu, Y. Xu, Y. Zhu, J. N. Culver, C. A. Lundgren, K. Xu and C. Wang, *ACS Nano*, 2013, **7**, 3627; (f) H. Zhu, Z. Jia, Y. Chen, N. Weadock, J. Wan, O. Vaaland, X. Han, T. Li and L. Hu, *Nano Lett.*, 2013, **13**, 3093.

10 (a) A. Darwiche, C. Marino, M. T. Sougrati, B. Fraisse, L. Stievano and L. Monconduit, *J. Am. Chem. Soc.*, 2012, **134**, 20805; (b) J. Qian, Y. Chen, L. Wu, Y. Cao, X. Ai and H. Yang, *Chem. Commun.*, 2012, **48**, 7070; (c) L. Baggetto, P. Ganesh, C.-N. Sun, R. A. Meisner, T. A. Zawodzinski and G. M. Veith, *J. Mater. Chem. A*, 2013, **1**, 7985; (d) W. Luo, S. Lorger, B. Wang, C. Bommier and X. Ji, *Chem. Commun.*, 2014, **50**, 5435; (e) X. Zhou, Z. Dai, J. Bao and Y.-G. Guo, *J. Mater. Chem. A*, 2013, **1**, 13727; (f) Y. Zhu, X. Han, Y. Xu, Y. Liu, S. Zheng, K. Xu, L. Hu and C. Wang, *ACS Nano*, 2013, **7**, 6378; (g) M. He, K. Kravchyk, M. Walter and M. V. Kovalenko, *Nano Lett.*, 2014, **14**, 1255.

11 (a) A. Darwiche, M. T. Sougrati, B. Fraisse, L. Stievano and L. Monconduit, *Electrochem. Commun.*, 2013, **32**, 18; (b) L. Ji, M. Gu, Y. Shao, X. Li, M. H. Engelhard, B. W. Arey, W. Wang, Z. Nie, J. Xiao, C. Wang, J.-G. Zhang and J. Liu, *Adv. Mater.*, 2014, **26**, 2901; (c) L. Xiao, Y. Cao, J. Xiao, W. Wang, L. Kovarik, Z. Nie and J. Liu, *Chem. Commun.*, 2012, **48**, 3321.

12 (a) M. Gu, A. Kushima, Y. Shao, J.-G. Zhang, J. Liu, N. D. Browning, J. Li and C. Wang, *Nano Lett.*, 2013, **13**, 5203; (b) D. Su, H.-J. Ahn and G. Wang, *Chem. Commun.*, 2013, **49**, 3131.

13 (a) B. Qu, C. Ma, G. Ji, C. Xu, J. Xu, Y. S. Meng, T. Wang and J. Y. Lee, *Adv. Mater.*, 2014, **26**, 3854; (b) X. Xie, D. Su, S. Chen, J. Zhang, S. Dou and G. Wang, *Chem. Asian J.*, 2014, **9**, 1611; (c) T. Zhou, W. K. Pang, C. Zhang, J. Yang, Z. Chen, H. K. Liu and Z. Guo, *ACS Nano*, 2014, **8**, 8323.

14 F. Klein, B. Jache, A. Bhide and P. Adelhelm, *Phys. Chem. Chem. Phys.*, 2013, **15**, 15876.

15 I. Lefebvre, M. A. Szymanski, J. Olivier-Fourcade and J. C. Jumas, *Phys. Rev. B*, 1998, **58**, 1896.

16 M.-Z. Xue, J. Yao, S.-C. Cheng and Z.-W. Fu, *J. Electrochem. Soc.*, 2006, **153**, A270.

17(a) C. Luo, Y. Xu, Y. Zhu, Y. Liu, S. Zheng, Y. Liu, A. Langrock and C. Wang, *ACS Nano*, 2013, **7**, 8003; (b) A. Abouimrane, D. Dambournet, K. W. Chapman, P. J. Chupas, W. Weng and K. Amine, *J. Am. Chem. Soc.*, 2012, **134**, 4505.

